

A Synchronous Investigation of Soil Geometric Mean Particle Diameter and Lime, Using Remote Sensing Technology (Case Study: Pol-e-Dokhtar, the Southwest of Lorestan Province, Iran)

M. Danesh¹, H. A. Bahrami^{1*}, S. K. Alavipanah², and A. A. Noroozi³

ABSTRACT

The geometric mean particle diameter (dg) and lime are two of the most important properties from the viewpoint of soil management. Nowadays remote sensing technology which has emerged walking with science development throughout the world, has made soil study faster, more facile and more cost-efficient. An investigation of soil dg and lime was performed in Pol-e-Dokhtar area by use of four sets of spectral data of IRS P₆, LISS III obtained from the Organizations of Geography of Armed Forces and Aerospace of Iran, in September 7th 2007. Subsequently, Principle Component Analysis, Normalized Difference Vegetation Index, Soil Line Euclidean Distance and Unsupervised Classification was carried out for satellite data sets following image preprocessing operations. Through stratified randomized sampling method and according to the false color composite and photomorphic units of the main image, 95 samples were selected and eventually collected from 0-5cm depth of soil surface, likewise 43 samples from 5-20cm. Afterwards, dg and lime contents were determined for each sampled point in soil laboratory. By means of multivariate regression operations there were eventually shown pronounced relationships ($P < 0.01$) between soil dg and lime with green ($R^2_{adj} = 0.78$) and NIR ($R^2_{adj} = 0.77$) bands in the first sampling depth. In addition, this was true for the second sampling depth with green ($R^2_{adj} = 0.57$), NIR ($R^2_{adj} = 0.55$) and red ($R^2_{adj} = 0.59$) bands with lower coefficients of determination. Consequently it has been substantiated with evidence that dg and lime contents are able to impress soil spectral reflectance. So it is possible to find out about these parameters using satellite and ancillary data.

Keywords: Geometric mean particle diameter, Normalized Difference Vegetation Index, Principle Component Analysis, Remote Sensing Technology, Soil lime.

INTRODUCTION

Soil is a heterogeneous system the processes and mechanisms of which are complex and difficult to fully comprehend. Many conventional soil analytical techniques are employed in an attempt to establish the relationship between soil physical and chemical properties and individual soil components, often

disregarding their complex, are multi-component interactions. Indeed, soil chemical extractions that unevitably alter the equilibrium between the phases may further complicate the interpretation of results. Historically, our understanding of the soil system and assessment of its quality and function has been gained through such types of laboratory analyses. We need to further develop our analytical techniques to better understand the soil as a complete system and

¹ Department of Soil Science, Faculty of Agriculture, Tarbiat Modares University, Tehran, Islamic Republic of Iran.

² Department of Remote Sensing and Cartography, Faculty of Geography, Tehran University, Tehran, Islamic Republic of Iran.

³ Soil Conservation and Watershed Management Research Institute, Tehran, Islamic Republic of Iran.

* Corresponding author; e-mail: bahramih@modares.ac.ir



a resource that we may make more efficient use of, and in the meantime preserve it for future generations. The acquisition of more accurate soil data is essential and more important now than ever before, if we are to manage our base resources sensibly to meet the food and fiber demands of future generations (Viscarra Rossel and McBratney, 1998a). On the other hand, spatial variation of agronomically significant soil attributes has become a subject of importance to the farming and to the wider communities (Larson and Robert, 1991; Robert *et al.*, 1995). Soil scientists have been challenged and as well aided during the past few decades by the simultaneous evolution and revolution in methods and instrumentations for soil data acquisition and modeling. A wealth of new soil information has become available to many countries (Baumgardner, 1999). In a lot of countries, in addition, substantial efforts have been devoted to the assessment of soil properties (mostly pertinent to the soil erodibility characteristics) (Bahrami *et al.*, 2005). The objective of these probes has been to give easily interpretable and spatially exhaustive information (principally in relation to land use and land evaluation) regarding soil properties. Anyhow soil information is needed at both regional and national scales to enable planning of land utilization in accordance with its capabilities. In the developed world, much effort is now being geared towards improving the existing soil information. The most efficient and cheapest means of achieving this is by studying soil reflectance which will be possible through remote sensing technologies (Odeh and McBratney, 2000). It is perhaps for these reasons that remote sensing techniques are being considered as possible alternatives (or surrogates) to enhance or replace conventional laboratory methods of soil analysis (Janik *et al.*, 1998). Remote Sensing (RS) has finally become an important tool to help evaluate environmental data. Spectral evaluation has proved to be useful particularly in characterizing and discriminating soils, mainly for survey

purposes (Demattê *et al.*, 2004). Remotely sensed data that can produce quantitative information on soil surface attributes would be useful supplements to traditional soil investigation for planning purposes. Such tools would also prove valuable in the emerging field of predictive soil studies (Scull *et al.*, 2003). The importance of spectral data on soil surveys has been demonstrated; however, detailed information on how to use soil reflectance in soil surveys is still lacking. Considering the importance of soil study in agriculture and environment, it is imperative to improve new methodologies using spectral data (Ben-Dor *et al.*, 1999).

Soil particle size is one of the most varied and consequential factors which influences soil chemical and physical properties (Means and Parcher, 1964). It is significantly related with texture and can affect soil structure, moisture, temperature, porosity, and compactibility (Folk, 1966; Campbell, 1985). Many important ecological and geomorphic processes in arid and semiarid area soils, including infiltration, physical crusting, pavement formation, and erodibility are affected and controlled by soil surface particle size (Ghorbani and Bahrami, 2005). The geometric mean diameter (dg) of soil particles, geometrically determines soil constituents' size which comprises important soil physical (mechanical) properties and which in turn are highly valued from the viewpoints of agricultural, bioenvironmental and engineering sciences (Bybordi, 2001). Several researchers have developed methods for mapping snow particle size using hyperspectral remote sensing (Nolin and Dozier, 2000; Painter *et al.*, 2003) and have shown the utility in a study of snow hydrology (Molotch *et al.*, 2003). Mineralogically, snow is much less complicated than most soils. However, the efforts of these authors (Molotch *et al.*, 2003) show that particle size can be retrieved using remotely sensed data, despite the sometimes-subtle effect it has on total pixel reflectance. Other investigators have

demonstrated that the spectral reflectance of bare soil surfaces depends on the effective particle size (Baumgardner *et al.*, 1985). Soil lime is as well another influential property which affects plant growth and nutrition (considering most soils in Iran being calcareous) (Malakouti, 2006). Nowadays the emerging remote sensing technology along with its contribution to soil science (Alavipanah, 2004) make investigations more facile and cost-efficient as compared to traditional methods (Alavipanah and Zehtabian, 2001; Nanni and Dematte, 2006). In accordance with recent investigations, maximum soil information will be obtained by studying spectral regions from visible to IR: 0.4-1.1 μm , SWIR (Shortwave Infrared): 1.1-2.5 μm and Thermal IR from 3-5 μm and 8-12 μm . (Swain and Davis, 1978; Glavao, 1998). Soil grain size can affect spectral scattering from soil surface (Baumgardner, 1985), that is, the smaller particles fill soil volume in an orderly manner and will cause even and smooth surfaces whereas the larger ones will cause rough and coarse surfaces leading to differentiation in spectral scattering from soil surface (Hoffer and Johannsen, 1969). Other investigators have demonstrated that the spectral reflectance of bare soils depends on the effective particle size (Baumgardner *et al.*, 1985). During a study in Mojave Desert by means of Airborne Visible Infrared Imaging Spectrometer (AVIRIS) and soil reflectance analysis methods, it was shown which soil grain size has a pronounced relationship with SWIR and changing of spectral reflectance versus grain size was led to changing of -0.06 in 1.7 μm (with $R^2= 0.89$) and -0.08 in 2.2 μm (with $R^2= 0.93$) of reflected spectrum for soil particle size estimation (Okin and Painter, 2003). Also shown is the possibility of getting access to significant information about soil carbonates by means of spectroscopic technology in Ultra Violet (UV) (250-400 nm), Visible (400-700 nm) and NIR (700-2,500 nm) ranges especially for soil lime in Visible and IR spectral regions (Islam *et al.*, 2003; Viscarra Rossel *et al.*, 2006). In addition, an

investigation fulfilled through laboratory spectroscopy methods has precisely estimated calcium carbonate content of soil samples in NIR and SWIR with an R^2 of about 0.95 (Gaffey, 1987). Anyway, this technique is non-destructive and therefore allows the preservation of the basic integrity of the soil system. Furthermore, using remotely sensed data allows for simultaneous characterization of various soil constituents. RS technique has advantages over some of the conventional techniques of soil analysis, e.g. this is rapid, timely and less expensive, hence more efficient when a large number of samples and analyses are involved. Moreover, it does not require expensive time-consuming sample pre-processing or the use of (environmentally harmful) chemical extractants. This paper presents an initial attempt of developing a rapid, cheap, accurate and non-destructive method to probe soil, using remotely sensed data. Here this investigation is extended to a simultaneous study of soil geometric mean diameter (dg) and lime (CaCO_3). This study examines the soil spectral properties as depicted by the IRS-P₆, LISS-III data set, with the main aim of developing measurement methods for improving soil attribute assessment in the Pol-e-Dokhtar of Lorestan Province, Iran. The study is also aimed at finding the most suitable relationships to enhance soil spatial prediction methods. Also the hypothesis was that soils would present differences in spectral reflectance due to their prevailing attributes especially geometric mean particle diameter (dg) and lime content and it was expected that the simultaneous assessment of soil and remotely sensed data would to some extent allow for a prediction of dg and lime at either one of the experimental depths.

Study Area

The investigation was conducted in the surroundings of Pol-e-Dokhtar, in the southwest of Lorestan Province, Iran (Figure

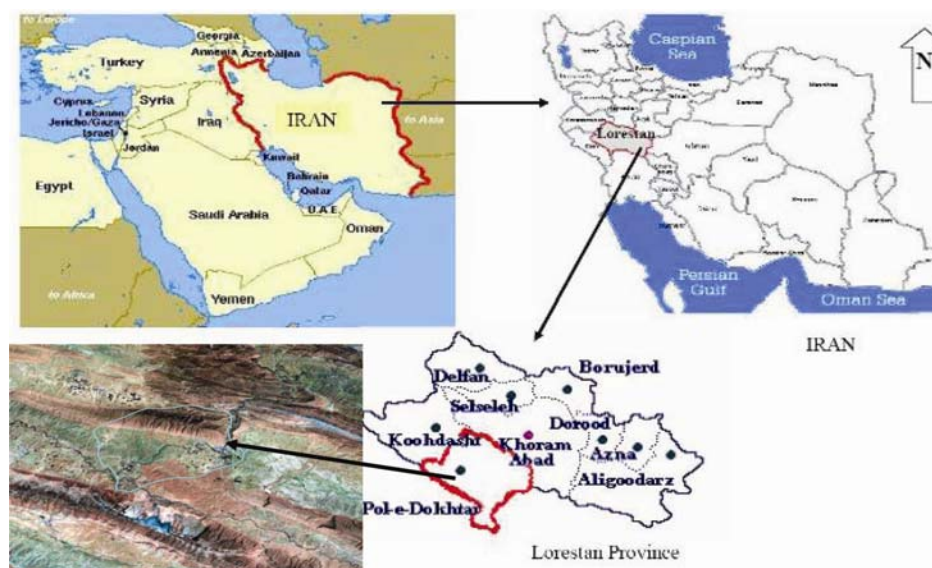


Figure 1. Geographic position of Pol-e-Dokhtar.

1). The study area extends over about 450 km² with a mean elevation of about 680 m and mean slope of about 26%. This region is also a part of Karkheh sub-basin and Kashkan basin with latitude of 33°3' to 33°15' and longitude of 47°29' to 47°44'. The climate of this region is arid to semiarid with mean temperature of the coldest (January) and warmest (August) months of about 9.8°C and 36.2°C respectively, mean annual precipitation of about 410 mm and 35% relative humidity (Alijani, 1995). The study region is covered by pastures and

sparse oak woods, scattered (dryland and irrigated) farmlands along with some rock outcrops in the middle parts. The most prevalent type of vegetation is *Astragalus amygdalus* which belongs to the arid regions. Also, the other types like *Festuca*, *Teucrium poliu*, *Euphorbia* and *Annualgrass sp.* have been observed.

MATERIALS AND METHODS

As mentioned earlier, the present study

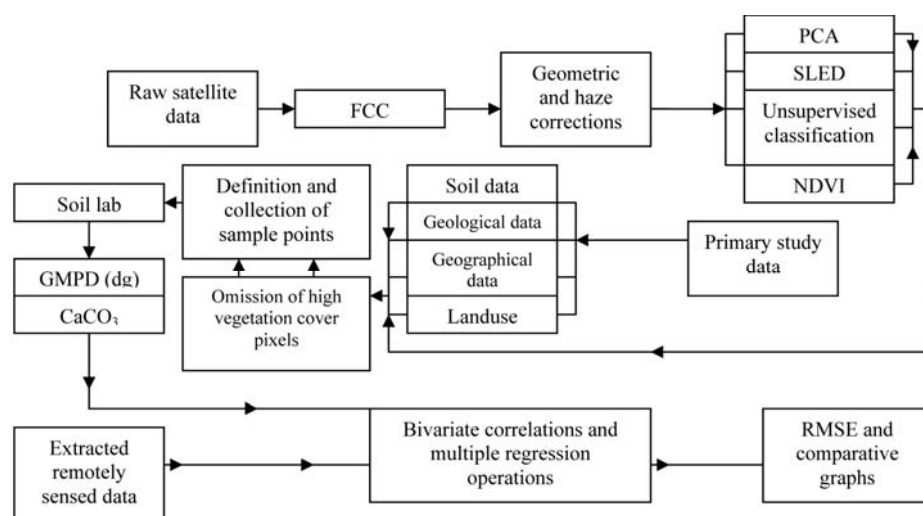


Figure 2. Overall stages of investigation process (in brief)

was conducted in the part of Kashkan sub-basin, nearby Pol-e-Dokhtar using a combination of field analyses, laboratory analyses as well as remotely sensed data. This research was fulfilled through data sets of IRS-P₆, LISS-III sensor of September 7th 2007, acquired from Organizations of Geography of Armed Forces and Aerospace of Iran, coincident with sample taking operations. Some characteristics of LISS-III sensor of IRS-P₆ are: 23.5m spatial resolution, 7 bit radiometric resolution and 140km imaging width. In addition, it comprises of 4 spectral bands of: green, red, near infrared and shortwave infrared. Data of spectral constituents were then put in ILWIS (Version 3.3) first and then tabulated to form a map list for satellite data so as to become prepared for preprocessing operations. Stages of the investigation process are briefly presented in Figure 2.

Data Processing

Initially, a coordinate system was determined for main image (Universal Transverse Mercator and Latitude-Longitude). The IRS-P₆, LISS III image was georeferenced by means of nearest neighbor resampling algorithm trained on more than 60 ground control points, obtaining a mean positional accuracy of about 0.5 pixel. This amendment (geometric correction) was made by means of digital maps of main roads and tracks of the study region in first spectral band (map to image method) and then it was subsequently done for other bands through the corrected image (image to

image method). To improve haze correction, the histogram of red band (second band) was plotted in such low land points of image as: river and ponds which had low digital numbers and explained nonnecessity of atmospheric correction for optical bands (Richards and Jia, 2005). Submap operations were then fulfilled for detaching of study region from the main image making it lucid for all bands. A map list of main bands was finally composed. Later, obtaining a complete and pure image of the study area, some processes were carried out consist of: NDVI (Normalized Difference Vegetation Index), PCA (Principal Component Analysis), USC (Unsupervised Classification) and SLED (Soil Line Euclidean Distance).

Determination of Sampling Points on the Study Region (Image)

A complete image reporting the spectral information regarding soil properties (geometric mean particle diameter and lime) was attained using data merging of five informative images comprised of:

- FCC (False Color Composite)

It was constructed by means of three regular bands (Gupta, 1991): red, green and NIR (2-1-3) in accordance with the best OIF (Optimum Index Factor): b_2, b_1, b_3 : 95.1. (Chavez *et al.*, 1982) (Figure 3-A).

PCA

To retain the most information in the data

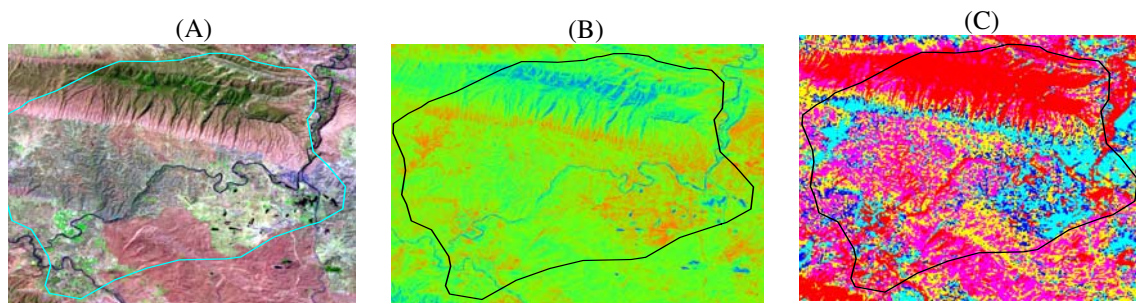


Figure 3A, B and C: A: FCC image of the study area, B: PCA₁ data layer and C: USC image of the study area.



while reducing the number of variables one must deal with PCA (Jensen, 1986). In other words that is a dimension reduction method that creates variables and increases data differentiation (Aitchison, 1986). PCA₁ (first layer) was formed by means of four spectral bands: green, red, NIR and SWIR (Figure 3-B)

USC

Cluster Analysis is a collection of techniques for aggregating objects into groups based on similarity measures or distances (dissimilarity). Unsupervised learning is learning without a priori knowledge about the classification of samples; learning without a teacher image (Lillesand and Kiefer, 1994). This process was executed in accordance with four bands and five clusters (because of lower accuracy of this image, it is only used for acquiring general information about the position of the region soil reflectance) (Figure 3-C).

SLED

The Soil Line Euclidean Distance technique relates a pixel's Euclidean Distance of the *R* and NIR to the *R* and NIR reflectance for the bottom most point on the soil line. It was done by means of red and NIR bands with the following formula (Fox and Sabbagh, 2002):

$$D = ((nir - A)^2 + (r - B)^2)^{0.5}$$

where *D* is the Euclidean Distance of each pixel from soil line, *nir* and *r* are respectively the spectral reflectance of NIR

and Red bands, while *A* and *B* are the minimum point reflectances of NIR and red bands (Figure 4-A)

NDVI

Most relationships linking soil features and surface reflectance are however indirect and complicated by the varying vegetation cover which masks the appearance of the underlying soil spectral properties (Murphy and Wadge, 1994). A visual examination of the study area image confirmed that the spectral responses of some areas were dominated by the presence of various extents of vegetation. Vegetation covers mask the most soil surface reflectance, hence some indices were needed to remove pixels of high vegetation cover to reduce sampling errors and this goal was aimed by use of NDVI of the following formula:

$$NDVI = (NIR - R) / (NIR + R)$$

in which NIR and *R* are the soil reflectances at these spectral regions (Bannari et al., 1995). This index has been the most commonly used vegetation index derived from remotely sensed data (Rondeaux et al., 1996) and is essentially an indicator of greenness cover of the land-surface (Huete, 1988) (Figure 4-B).

Sample points were eventually determined on the basis of all acquired data specially FCC (because it shows the soil surface features more clearly, distinct and actual). Subsequently through addition of SLED and PCA₁ data layer and as well the auxiliary data layers of the study region like: land use, soil series, rivers and ponds, tracks and roads, to the base image about 95 points were settled by way of stratified randomized

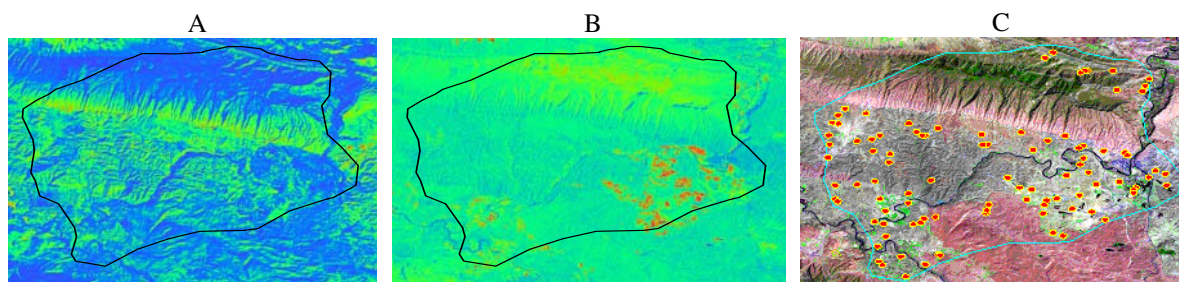


Figure 4- A, B and C: SLED image of the study area, B: NDVI data layer and C: Positions of sampling points

sampling method (Khajehdin, 2001) with an extensive distribution over region image (Figure 4-C). Latitudes and longitudes for each sample point were then clarified and extracted in ILWIS.

Sampling

After determining sampling points and their characteristics over the image (stratified random sampling), the sites of samples were found through GPS in the study area. Samples were collected from two depths in undisturbed soils (0-5 cm and 5-20 cm) and one from surface soil (0-5 cm) in disturbed soils (due to successive plowing and other farming operations). At last 95 samples were collected from 0-5 and 43 from 5-20 cm.

Laboratory Operations

After conveying pockets of collected samples from Pol-e-Dokhtar to the soil lab (Faculty of Agriculture, Tarbiat Modares University), samples were air-dried, crushed and sieved using a brass sieve of 2 mm openings. The < 2 mm fraction was taken for laboratory analyses. Such analyses as: particle size distribution (hydrometric procedure), calcium carbonate (HCl solution and NaOH titration method) (Weaver and Angle, 1994), and moisture content (by weighing procedure) were made for each soil sample (procedures described by Soil Survey Staff (1996)).

Calculations

Since soil texture is an indication of frequency and numeral mean diameter of soil particles, it is possible *via* soil textural triangle of Shirazi and Boersma (1984) to have access to important information regarding grains geometric diameter and soil mechanical analysis (Bybordi, 2001). For an investigation of the effect of geometric mean

particle diameter (dg) on the soil spectral reflectance, the quantity of each soil component (texture) has been converted to the geometric mean particle diameter using the following formula presented by Shirazi

$$a = 0.01 \sum_{i=1}^n f_i \ln M_i \longrightarrow dg = exp$$

and Boersma (1984):

in which dg represents geometric mean diameter, f_i is frequency percentage of each fragment (sand, silt and clay) and M_i is numeral mean diameter of each component (for sand= 1.025, silt= 0.026, and clay= 0.001 mm).

Pearson's two-tailed correlations (bivariate) between soil acquired data and remotely sensed data of four spectral bands, PCA₁ and SLED were calculated and their scatter plots were delineated for all samples in Statistical Package for Social Sciences (SPSS Inc., 2004). Regression equations were subsequently obtained and accuracy tested for each relationship through control samples if there was a pronounced correlation (at either 0.01 or 0.05 probability level). Thenceforth remotely sensed data of sample points in: four bands (red, green, NIR and SWIR), PCA₁, SLED and soil laboratory data of representative sample points: geometric mean particle diameter (dg) and lime (CaCO₃) contents were introduced into the SPSS to drawing their scatter plots and finding out the correlation matrices between attained satellite and terrestrial data. Best relations were at last defined for significant correlations and their precision tested and verified according to the representative samples (10 samples from the first depth and 5 ones from the second depth) by means of Root Mean Square Error (RMSE) and Graph Conformance (GC), performed in MATLAB (Matlab, Ver. 7.1, 2006) and Excel.

RESULTS AND DISCUSSION

Correlation matrices (and scatter plots) were used for studying the relationships

**Table 1.** Correlations between soil information and satellite data in two sampling depths.

	Gr	R	NIR	SWIR	PC1	SLED
dg(0-5 cm)	0.753**	0.684**	0.568**	0.586**	0.692**	0.023
CaCO ₃ (0-5 cm)	-0.625**	-0.611**	-0.716**	-0.572**	-0.651**	-0.002
dg(5-20 cm)	0.663**	0.652**	0.592**	0.525**	0.642**	-0.037
CaCO ₃ (5-20 cm)	-0.578**	-0.619**	-0.604**	-0.543**	-0.606**	-0.098

** Significant at 0.01 probability level.

between soil and satellite data the principal results of which are briefly shown in the table that follows (Table 1). Considering the first depth samples, maximum correlation exists between dg and green band ($R= 0.753$). There was a significant correlation observed between dg and PCA₁ ($R= 0.692$) while, there was no meaningful relationship existing between dg and SLED. As well, lime shows a noticeable correlation with NIR ($R= - 0.716$) and then with PCA₁ ($R= - 0.651$), whereas there was no important correlation seen with SLED (same as for dg). For the second depth, correlations were found out as well: dg with green and PCA₁ with $R= 0.663$ and 0.642 respectively, CaCO₃ with red and PCA₁ with $R= -0.619$ and -0.606 respectively. Furthermore, geometric mean particle diameter (dg) and calcium carbonate values also exhibited relatively considerable correlations ($R= 0.557$ for the first and 0.526 for the second depth). This relationship was inverse between CaCO₃ and geometric mean particle diameter.

Therefore it is evident that dg and lime of the studied region have pronounced impact on spectral bands (green, red and NIR) and on PCA₁. Hence it is possible to investigate them utilizing satellite data. For more precision one should use data bands with higher correlation coefficients (r) than others. Therefore green, NIR and red bands were selected to study soil characteristics of both depths because of higher correlations with dg and CaCO₃. Also PCA₁ has a good relationship with soil data as compared with SLED. It is indicated that all relationships in the first depth follow third degree functions (nonlinear) superiorly and then linear equations with lower R^2 s (coefficients of determination) are defined too. Because of

synchronous effect of soil mentioned properties (GMPD and lime) on its spectral reflectance, an access to the relationships is therefore feasible by multivariate regression operations. Multivariate regressions (nonlinear as well as linear) between soil information and remotely sensed data were mathematically computed. According to the coefficient of determination (R^2), adjusted R^2 and standard errors of the estimate of acquired equations, the most proper relations were eventually defined. Later GMPD (dg) and lime contents of samples were estimated by means of attained regressions and then compared with those in the representative samples for accuracy evaluation. Equation accuracies were testified by way of RMSE and GC in MATLAB and EXCEL. Attained relations are as follows:

1). Nonlinear equation (third degree) of geometric mean diameter (dg) and lime (CaCO₃) with green and NIR bands for samples of the first depth:

$$\text{Gr}=102.18+785.39X-4258.34X^2+11252.87X^3+.035Y^2-.001Y^3-5.63XY, R^2_{\text{Gr}}= 0.775$$

$$\text{NIR}=183.61+229.22X-592.4X^2-7.214Y+.23Y^2-.002Y^3, R^2_{\text{NIR}}= 0.767$$

On the basis of these equations, X values (dg) were estimated through RMSE about 0.02295 and Y values (CaCO₃) about 5.24 with either graph conformities shown in Figures 5-A₁ and A₂.

2). Nonlinear equation (third degree) of geometric mean diameter (dg) and lime (CaCO₃) with green and red bands for samples of the soil second depth:

$$\text{Gr}= 230.014+265.646X-8.998Y+.241Y^2-.002Y^3, R^2_{\text{Gr}}= 0.571$$

$$\text{R}= 238.39+287.74X-9.54Y+.26Y^2-.002Y^3, R^2_{\text{R}}= 0.593$$

According to these equations, X (dg) and Y (CaCO_3) contents were estimated through RMSE about 0.0480 and 9.75 respectively. Their comparing graphs are shown in Figures 5-B₁ and B₂.

3). Geometric mean diameter (dg) and lime relationships with PCA_1 for the first depth:

$$\text{PC1}=402.82-15.22Y+4.466Y^2-.005Y^3, \\ R^2_{\text{PC1}}=0.559$$

$$\text{PC1}=184.49-1491.85X- \\ 8942.93X^2+23670.51X^3+.075Y^2-.002Y^3- \\ 10.06XY, R^2_{\text{PC1}}=0.761$$

Using the first equation, Y contents (CaCO_3) were estimated and put into the second equation. Hence X contents (dg) were estimated through RMSE about 0.0359 and Y (CaCO_3) estimated through RMSE close to 7.55. Comparison graphs are presented in the Figures 5-C₁ and C₂.

4). Geometric mean diameter (dg) and lime relationships with PCA_1 for the second depth:

$$\text{PC1}=210.884+547.74X, R^2_{\text{PC1}}=0.392$$

$$\text{PC1}=400.729+441.08X- \\ 15.146Y+.416Y^2+.004Y^3, R^2_{\text{PC1}}=0.577$$

In accordance with these equations, X (dg) and Y (CaCO_3) contents were calculated through RMSE as approximately 0.033 and 7.57 respectively. Graphs are shown in Figures 5-D₁ and D₂.

5). Linear equation of dg and CaCO_3 with green and NIR bands for the first depth:

$$\text{Gr}=142.93+222.95X-.785Y, R^2_{\text{Gr}}=0.683$$

$$\text{NIR}=154.7-1.365Y+3.913XY, R^2_{\text{NIR}}= \\ 0.602$$

On the basis of these equations X (dg) and Y (CaCO_3) contents were calculated through RMSE 0.0517 and 9.88 respectively. Graphs

are presented in Figures 5-E₁ and E₂.

6). Linear equation of dg and CaCO_3 with green and red bands for the second depth:

$$\text{Gr}=150.72+257.1X-.878Y, R^2_{\text{Gr}}=0.546$$

$$\text{R}=172.55-1.447Y+9.357X, R^2_{\text{R}}=0.537$$

According to these equations X (dg) and Y (CaCO_3) values were estimated through RMSE as 0.0348 and 9.45 respectively. Comparative graphs are presented in the Figures 5-F₁ and F₂.

After statistical and mathematical analyses (through multivariate regression functions) being carried out for soil parameters and satellite data, it was proved that dg and lime of the soil surface layer (first depth) had pronounced correlations ($P \leq 0.01$) with major spectral bands (especially green and NIR) and PCA_1 . Correlations were of a slightly lower degree for the second sampling depth but yet they were significant. Hence it is possible to investigate these soil properties simultaneously by means of LISS-III, IRS-P₆ data set in this region. On the basis of the comparative graphs (Figures 5 and 6) and RMSEs (Table 2) it is evident the best estimation of soil properties in the surface layer (0-5 cm) can be made respectively by the: cubic relations of green and NIR bands, PCA_1 and then linear relations of green and NIR bands. Likewise for the second depth (5-20 cm) the best equations would respectively: PCA_1 equations, linear relations and then cubic (nonlinear) equations (Table 2). As can be seen A, B, C and D graphs of Figure 6, express priority and precedence among the attained

Table 2. RMSEs of equations for two sampling depths.

	First depth (0.5 cm)			Second depth (5-20 cm)		
	Cubic relation	Linear relation	PCA_1 relation	Cubic relation	Linear relation	PCA_1 relation
dg	0.02291	0.05165	0.03598	0.0480	0.03486	0.03276
CaCO_3	5.24	9.88	7.54	9.74	9.45	7.57

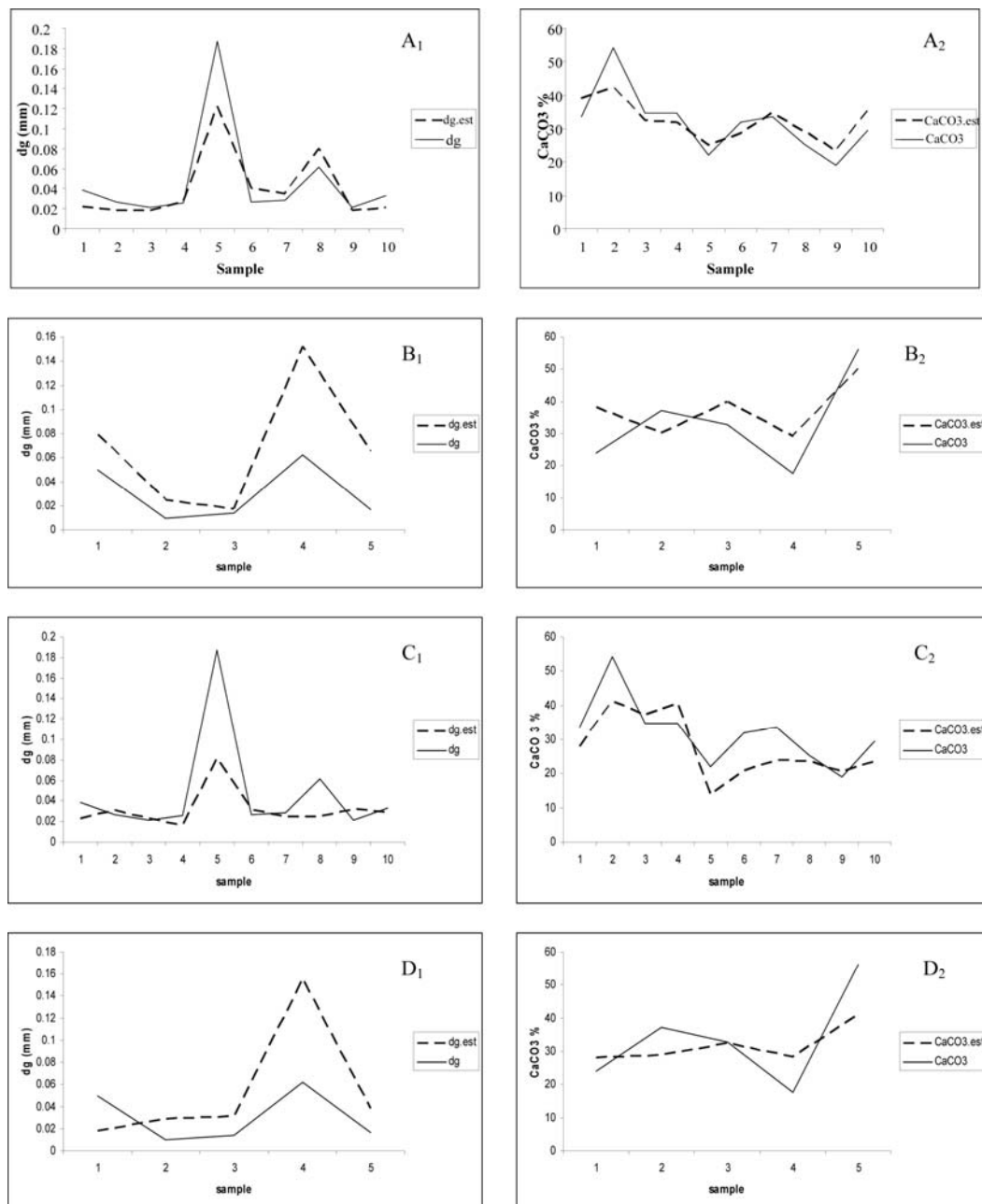


Figure 5. Comparative graphs of estimated values through equations versus measured values in the laboratory (Y-axis: dg and lime content; X-axis: Representative samples).

- (A₁) dg.est: Estimated dg by (nonlinear) cubic relations; dg: Determined dg by lab. methods, for the first depth.
(A₂) CaCO₃.est: Estimated lime by cubic relation; CaCO₃: Determined lime by lab. methods, for the first depth.
(B₁) dg.est: Estimated dg by (nonlinear) cubic relations; dg: Determined dg by lab. methods, for the first depth.
(B₂) CaCO₃.est: Estimated lime by cubic relation; CaCO₃: Determined lime by lab. methods, for the first depth.
(C₁) dg.est: Estimated dg by PCA relation; dg: Determined dg by lab. Methods, methods, for the first depth.
(C₂) CaCO₃.est: Estimated lime by PCA relation; CaCO₃: Determined lime by lab. methods, for the first depth.
(D₁) dg.est: Estimated dg by PCA relation; dg: Determined dg by lab. methods, for the first depth.
(D₂) CaCO₃.est: Estimated lime by PCA relation; CaCO₃: Determined lime by lab. methods, for the first depth.
(E₁) dg.est: Estimated dg by linear relations; dg: Determined dg by lab. methods, for the first depth.
(E₂) CaCO₃.est: Estimated lime by linear relations; CaCO₃: Determined lime by lab. methods, for the first depth.
(F₁) dg.est: Estimated dg by linear relations; dg: Determined dg by lab. methods, for the first depth.
(F₂) CaCO₃.est: Estimated lime by linear relations; CaCO₃: Determined lime by lab. methods, for the first depth.
Continued.

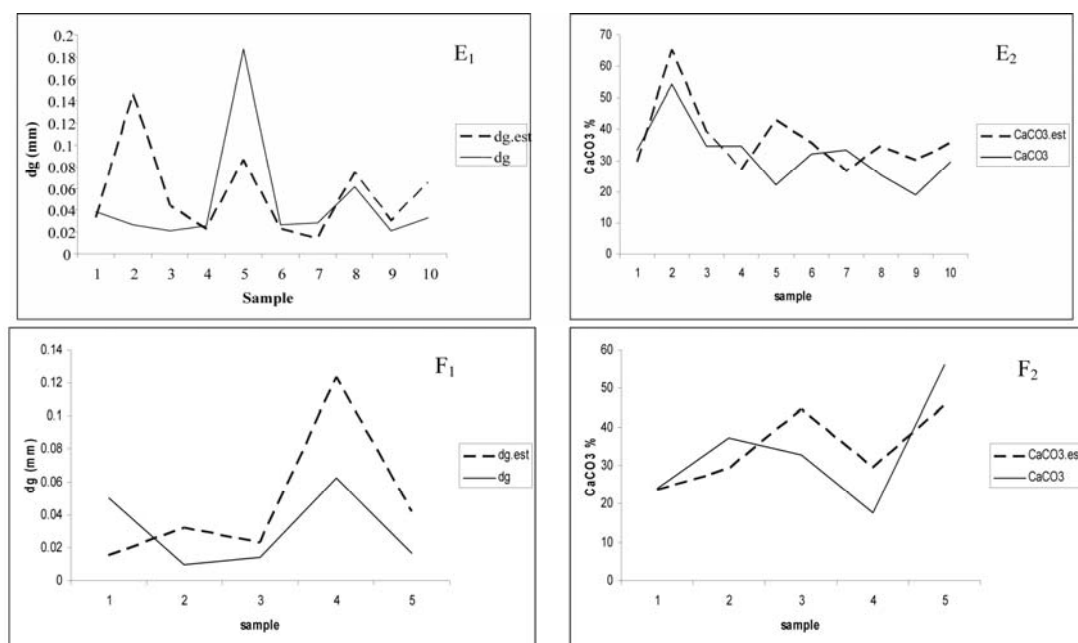


Figure 5. continued

equations for estimating soil geometric mean particle diameter and lime decided by the quantities found out in the soil lab.

In Figure 6 $dg.cub$, $dg.lin$, $dg.pc$ and dg represent the estimated dg through: third degree equations, linear equations, PCA_1 relations and the determined quantities in the lab respectively. Also $CaCO_3.cub$, $CaCO_3.lin$, $CaCO_3.pc$ and $CaCO_3$ are the estimated quantities of $CaCO_3$ through: third degree equations, linear equations, PCA_1 relations and the determined figures in the lab respectively.

It has consequently been proved that there is a significant and considerable impression of soil geometric mean particle diameter and lime on the soil spectral reflectance in the Pol-e-Dokhtar area. In other words, soil reflectance in this region, which is predominantly mirroring, contains important data concerning soil properties (dg and lime) and it is almost certain that one is able to study these parameters *via* utilizing the information obtained through remotely sensed techniques.

CONCLUSION

The current investigation was aimed at developing and examining a methodology to

simultaneously investigate soil geometric mean particle diameter and lime by use of remotely sensed data. Hence, the possibility of using optical satellite images to extend sample points over the study region was fulfilled. Some areas with high vegetation cover were not selected for sampling while using NDVI over the satellite image. The methodology is briefly composed of following operations:

- 1). Use of PCA, SLED and USC operations over the remotely sensed data.
- 2). A determining of sampling points on the basis of the FCC and soil ancillary data in the study region.
- 3). Studying the relationships between soil (geometric mean particle diameter and lime) and remotely sensed data (four satellite spectral bands, PCA_1 , SLED) over the selected points.
- 4). Clarifying the precision and accuracy of the achieved relationships.

The study has demonstrated the potential for using the IRS-P₆, LISS-III data for spatial prediction of soil attributes (dg and lime) that are in high correlation with the spectral reflectance of soil surface. The study is considerably pertinent to the remotely sensed data which are ubiquitous

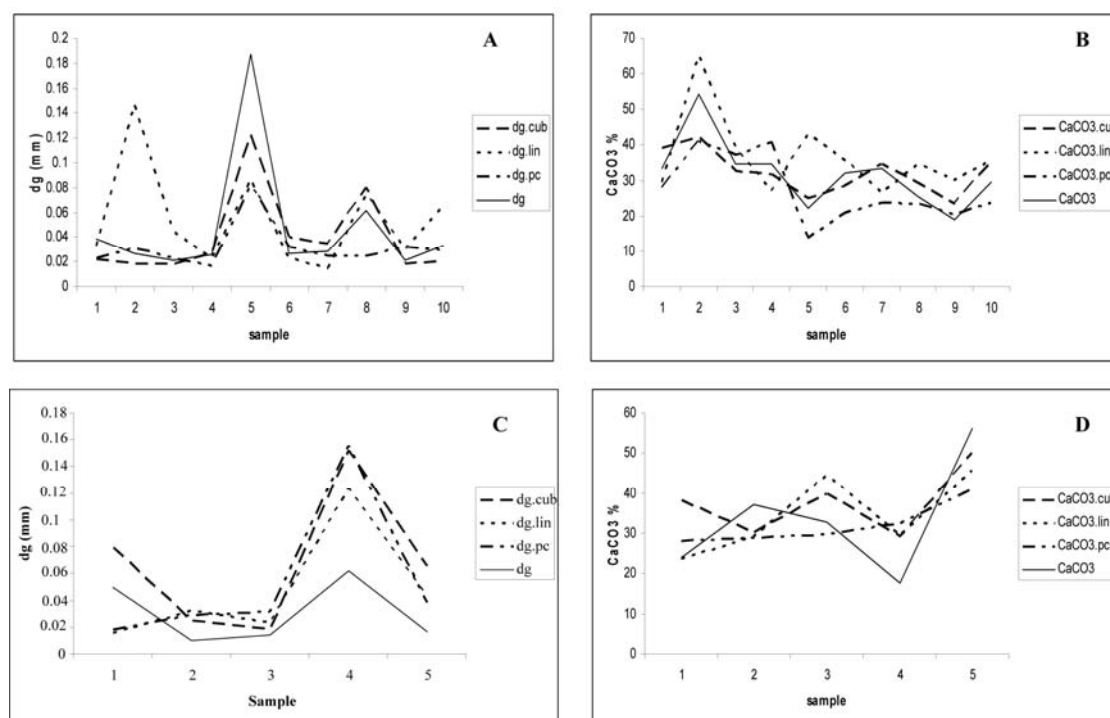


Figure 6. Obtained values using estimative equations in contrast to main amounts using soil lab

operations.

(A): Comparison of acquired equations for dg estimation for the first depth.

(B): Comparison of acquired equations for CaCO₃ estimation for the first depth.

(C): Comparison of acquired equations for dg estimation for the first depth.

(D): Comparison of acquired equations for CaCO₃ estimation for the first depth.

and of the capability to cover extensive areas. Moreover, it was indicated that using distantly sensed data may improve the soil predictability of the geometric mean particle diameter as well as lime with relatively admissible accuracy. In conclusion, the following findings are obtained from the study:

-Green and NIR bands have satisfactory correlations with soil GMPD (dg) and lime, therefore a use of these spectral bands would improve the soil attribute prediction power.

-PCA₁ has also proved slightly suitable in probing the topsoil GMPD and lime.

-SLED was found as inconsiderable in this investigation.

-The prediction relationship that best incorporates the remotely sensed information and soil data is a combination of nonlinear (cubic) multiple regressions rather

than linear multiple regression (for the topsoil).

-The best relationship for the second sampling depth is linear rather than nonlinear multiple regression.

The ability to retrieve information on soil geometric mean particle diameter and lime in arid and semiarid regions has a wide range of applications in ecological and geomorphological sciences. Extensive research is still required before a method for retrieval of these factors, using RS, will be possible. In particular, the results indicate that dg and lime exert influence on spectral shape of soils which can be sensed through satellites. Further research is indispensable to quantify the effect of these factors on spectral reflectance. Nonetheless, this study shows that soil geometric mean diameter and lime do impact apparent surface reflectance in a way that is measurable by

Table 3. The attained R^2 (adjusted) values of multiple regression equations for either one of the sampling depths.

	First sampling depth (0-5 cm)			Second sampling depth (5-20 cm)		
	Cubic relation	Linear relation	PCA ₁ relation	Cubic relation	Linear relation	PCA ₁ relation
Average adjusted R^2	0.771	0.642	0.660	0.582	0.541	0.484

timely remotely sensed data, and thus opens the door for the development of remote sensing methods for soil property retrievals. In turn, the dg and lime retrievals will facilitate quantitative spatial modeling of landscape processes in the studied environments. Increase of depth from soil surface promoted a reduction in the magnitude of correlation of soil samples and remotely sensed data meaningfully. Also it was found out that as soil-dg increases, remotely sensed DNs also increase (positive correlation). Conversely, as soil lime content increases, a decrease is observed in the remotely sensed DNs (negative correlation). Taken together, this study provided some valuable information to research in the context of geometric mean particle diameter and lime content of the soil using the spectral data which that were remotely sensed. In this investigation, it was found that such remote sensing technique as SLED had no relationship with soil dg and lime. It is eventually possible to estimate soil geometric mean diameter and lime content by using a multiple regression model of the dimensions of the soil and remotely sensed data in this region. The multiple regression relations developed in this study reached an R^2 value of 0.77 for cubic relations for the first sampling depth. R^2 values of the achieved equations are shown in Table 3.

The work presented here provides a starting point on which future research in soil geometric mean particle diameter and lime may be based. Further experimentation is needed to improve measurements and verification. It is worth mentioning that soil

moisture has exerted an attenuated influence on spectral reflectance in this study, because of time of field sampling (September) and regarding the fact that during the summer season the average rainfall is near 0 mm in the study region. Hence it has had a negligible effect on soil reflectance during the study. In addition, obtained multiple regressions for simultaneous estimations of geometric mean particle diameter and lime may be useful and feasible for similar semi-arid and arid zones where vegetation is either scant or absent during some periods of the year when the soil moisture is at its least.

ACKNOWLEDGEMENTS

The authors are grateful to Dr. Malekimoghaddam for his keen review and as well to Dr. Tahmasebipoor and to the Department of Pasture and Watershed Management of Pole-Dokhtar for their helpful collaborations. They would also like to extend their thanks to Organization of Geography of Armed Forces and Aerospace Organization of Iran, for providing satellite images employed in the probe.

REFERENCES

1. Aitchison, J. 1986. *The Statistical Analysis of Compositional Data*. Chapman and Hall, New York.
2. Alavipanah, S. K. 2004. *Application of Remote Sensing in the Earth Sciences (Soil)*. University of Tehran Press, PP. 28-33. (In Persian)



3. Alavipanah, S. K. and Zehtabian, G. R. 2001. Remote Sensing and GIS Tools for Landuse Planning and Management. Proceedings of the FIG Working Week 2001 (FWW 2001), May 6-11 2001, Seoul, Korea.
4. Alijani, B. 1995. *Climatology of Iran (Geography)*. Publication of Payame Noor, Tehran, Iran. (In Persian)
5. Bahrami, H. A., Pornalkh, T. and Tahmasebipoor, N. 2005. Study of Soil Erodibility in Different Land Uses from Chamanjir Watershed. *Proc. of the Third National Conf. of Erosion and Sediment*, Tehran, PP. 505-510. (In Persian)
6. Bannari, A., Morin, D., Bonn, F. and Huete, A. R. 1995. A Review of Vegetation Indices. *Remote Sensing Reviews*, **13**: 95-120.
7. Baumgardner, M. F., Silva, L. F., Biehl, L. L. and Stoner, E. R. 1985. Reflectance Properties of Soil. *Adv. Agron.*, **38**: 1- 44.
8. Baumgardner, M. F. 1999. Soil Databases. In: "*Handbook of Soil Science*", Summer, M. E. (Ed.), printed in the USA, ISBN: 0-8493-3136-6 PP. H1-H3
9. Ben-Dor, E., Irons, J. R. and Epema, G. F. 1999. Soil Reflectance, 3rd Edition. In: "*Remote Sensing for the Earth Sciences*", Rencz, A. N. (Ed.). *Manual of Remote Sensing*, **3**: 111- 188.
10. Bybordi, M. 2001. *Soil Physics*. 6th Edition, No. 1672, Tehran University Publications, PP. 567-574. (In Persian)
11. Campbell, G. S. 1985. *Soil Physics with BASIC*. Elsevier, Amsterdam.
12. Chavez, P.S., Berlin, G. L. and Sowers, L. B. 1982. Statistical Methods for Selecting Landsat-MSS Ratios. *J. Appl. Photogramm. Eng.*, **8(1)**: 23-30.
13. Demattê, J. A. M., Campos, R. C., Alves, M. C., Fiorio, P. R. and Nanni, M. R. 2004. Visible-NIR Reflectance: A New Approach on Soil Evaluation. *Geoderma*, **121**: 95-112.
14. Folk, R. L. 1966. A Review of Grain Size Parameters. *Sedimentology*, **6**: 73-93.
15. Fox, G. A. and Sabbagh, G. J. 2002. Estimation of Soil Organic Matter from Red and Near-Infrared Remotely Sensed Data Using a Soil Line Euclidean Distance Technique. *Soil Sci. Soc. Am. J.*, **66**: 1922-1928.
16. Gaffey, S. J. 1987. Spectral Reflectance of Carbonate Minerals in the Visible and Near Infrared (0.35-2.55 μm): Anhydrous Carbonate Minerals. *J. Geophys. Res.*, **92**: 1429-1440.
17. Ghorbani, H. and Bahrami, H. A. 2005. Assessment of Soil Erodibility by Weight Method in USLE and RUSLE Using GIS in Northeast Lorestan Province. *Proceedings of the Third National Conference of Erosion and Sediment*, Tehran, PP. 658-660. (In Persian)
18. Glavao, L. S. and Vitorello, I. 1998. Variability of Laboratory Measured Soil Lines of Soil from Southeastern Brazil. *Remote Sens. Environ.* **6**: 166-181.
19. Gupta, R. D. 1991. *Remote Sensing Geology*. Springer Verlag Publications, 365 PP.
20. Hoffer, R. M. and Johannsen, C. J. 1969. Ecological Potentials in Spectral Signatures Analysis. In: "*Remote Sensing in Ecology*", Johnson, P. L. (Ed.). University of Georgia Press, Athens, USA.
21. Huete, A. R. 1988. A Soil-Adjusted Vegetation Index (SAVI). *Remote Sens. of Environ.*, **25**: 295-309.
22. ILWIS, 2005. *ILWIS*. Version 3.3, Academic, ITC (RSG/GSD), The Netherlands.
23. Islam, K., Singh, B. and McBratney, A. B. 2003. Simultaneous Estimation of Various Soil Properties by Ultra-Violet, Visible and Near-Infrared Reflectance Spectroscopy. *Aust. J. Soil Res.*, **41**: 1101-1114.
24. Janik, L. J., Merry, R. H. and Skjemstad, J. O. 1998. Can Mid Infra-Red Diffuse Reflectance Analysis Replace Soil Extractions?. *Aust. J. Exp. Agric.*, **38(7)**: 681- 696.
25. Jensen, J. R. 1986. Introduction Digital Image Processing: A Remote Sensing Perspective. Cliffs, New Jersey, 379 PP.
26. Khajehdin, S. J. 2001. Data Collecting Methods for Satellite Data Interpretation. *Papers Collection of First Congress of Desertification and Its Cure*, Forest and Pastures Research Institute, PP. 337-338. (In Persian)
27. Larson, W. E. and Robert, P. C. 1991. Farming by Soil. In: "*Soil Management for Sustainability*", Lal, R. and Pierce, F. J. (Eds.). *Soil Water Conserv. Soc.*, Ankeny, **IA**: 103-120.
28. Lillesand Thomas, M. and Kiefer Plaph, W. 1994. *Remote Sensing and Image Interpretation*. John Willey and Sons, Inc.
29. Malakouti, M. J. 2006. A Look at the Fertility Status of Iranian Soils (Evaluation

- and Utilization). Sana Publications, PP. 183-184. (In Persian)
30. MATLAB, 2006. *MATLAB*. Version 7.1, The Math. Works, Inc., 24 Prime Park Way, Natick, Massachusetts 01760, USA.
 31. Means, R. E. and Parcher, J. V., 1964. *Physical Properties of Soils*. Publication of Charles E. Merrill Books Inc. PP. 464
 32. Molotch, N., Painter, T. H., Bales, R. and Dozier, J. 2003. Incorporating Remotely Sensed Snow Albedo into a Spatially Distributed Snowmelt Model. In review *Geophysical Research Letters*.
 33. Murphy, R. J. and Wadge, G. 1994. The Effects of Vegetation on the Ability to Map Soils Using Imaging Spectrometer Data. *Int. J. Remote Sens.*, **15(1)**: 63-86.
 34. Nanni, M. R. and Dematte, J. L. M. 2006. Spectral Reflectance Methodology in Comparison with Traditional Soil Analysis. *Soil Sci. Soc. Am. J.*, **70**: 393-407.
 35. Nolin, A. W. and Dozier, J. 2000. A Hyperspectral Method for Remotely Sensing the Grain Size of Snow. *Remote Sens. Environ.*, **74(2)**: 207-216.
 36. Odeh, I. O. A. and McBratney, A. B. 2000. Using AVHRR Images for Spatial Prediction of Clay Content in the Lower Namoi Valley of Eastern Australia. *Geoderma*, **97**: 237-254.
 37. Okin, G. S. and Painter, T. H. 2003. Effect of Grain Size on Remotely Sensed Spectral Reflectance of Sandy Desert Surfaces. *Remote Sens. Environ.*, **89**: 272-280.
 38. Painter, T. H., Dozier, J., Roberts, D. A., Davis, R. E. and Green, R.O. 2003. Retrieval of Subpixel Snow-Covered Area and Grain Size from Imaging Spectrometer Data. *Remote Sens. Environ.*, **85**: 64-77.
 39. Richards, J. A. and Jia, X. 2005. Remote Sensing Digital Image Analysis: An Introduction (pp. 439). (Fourth edition). Berlin: Springer-Verlag and Szabolcs, I. (2005). Salt Affected Soils in Europe (pp. 439). The Hague: Martinus Nijhoff.
 40. Robert, P. C., Rust, R. H. and Larson, W. E. 1995. *Site-Specific Management for Agricultural Systems*. American Society of Agronomy, Madison, WI.
 41. Rondeaux, G., Steven, M. and Baret, F. 1996. Optimization of Soil-Adjusted Vegetation Indices. *Remote Sens. Environ.*, **55**: 95-107.
 42. Scull, P., Franklin, J., Chadwick, O. A. and McArthur, D. 2003. Predictive Soil Mapping: A Review. *Progress in Physical Geography*, **27(2)**: 171-197.
 43. Shirazi, M. A. and Boersma, L. 1984. A Unifying Quantitative Analysis of Soil Texture. *Soil Sci. Soc. Am. J.*, **48**: 142-147.
 44. *Soil Studies of the Karkheh Basin (The Diagnostic and Supplementary Studies on Karkheh Basin)*, 1995. The Construction Jihad Office of Lorestan Province, Khoram Abad, Iran. (In Persian)
 45. Soil Survey Staff, 1996. *Soil Survey Laboratory Methods Manual*. Version 3.0, Soil Survey Investigations Report No. 42, USDANRCS National Soil Survey Center, Washington, D.C.
 46. SPSS, 2004. *Statistical Package for the Social Sciences*. Version 13.0, SPSS Inc., Apache Software Foundation.
 47. Swain, P. H. and Davis, S. M. 1978. *Remote Sensing: The Quantitative Approach*. McGraw Hill, New York.
 48. Viscarra Rossel, R. A. and McBratney, A. B. 1998a. Soil Chemical Analytical Accuracy and Costs: Implications from Precision Agriculture. *Aust. J. Exp. Agric.*, **38**: 765-775.
 49. Viscarra Rossel, R. A., Walwoort, D. J. J., McBratney, A. B., Janik, L. K. and Skjemstad, J. O. 2006b. Visible, Near Infrared, Mid-Infrared or Combined Diffuse Reflectance Spectroscopy for Simultaneous Assessment of Various Soil Properties. *Geoderma*, **131**: 59-75.
 50. Weaver, R. W. and Angle, J. S. 1994. *Methods of Soil Analysis, Microbiological and Biochemical Properties*. Part II, Soil Sci. Soci. Am. NC, USA.



بررسی همزمان میانگین هندسی قطر ذرات و آهک خاک با استفاده از فناوری سنجش از دور (مطالعه موردی: جنوب غربی استان لرستان، منطقه پل دختر)

م. دانش، ح.ع. بهرامی، س. ک. علوی پناه و ع. ا. نوروزی

چکیده

میانگین هندسی قطر ذرات و آهک خاک از پارامترهای مهم خاک بوده که اطلاع از وضعیت آنها از نظر مدیریت خاک بسیار مهم می‌باشد. امروزه با ظهور فناوری سنجش از دور، امکان بهره برداری از این فناوری در علوم خاک جهت مطالعه ویژگی های خاک از جمله اندازه هندسی ذرات و آهک خاک، با صرف وقت و هزینه کمتری، فراهم گشته است. برای مطالعه این دو خصوصیت خاک در منطقه پل دختر، از داده های چهار طیفی ماهواره IRS-P₆ سنجنده LISS III و در تاریخ ۱۷ شهریور ماه سال ۱۳۸۶ استفاده گردید. پس از بدست آوردن تصویر منطقه، تصحیحات لازم (هندسی) بر روی آن انجام گرفت و سپس پردازشهایی شامل: PCA، NDVI، SLED و USC انجام شد. در نهایت با استفاده از روش نمونه برداری طبقه بندی شده تصادفی و بر اساس FCC و PMU در تصویر اصلی و لایه های اطلاعاتی، ۹۵ نقطه تعیین و از دو عمق ۵-۰ و ۲۰-۵ سانتیمتری سطح خاک نمونه برداری انجام گردید. با استفاده از رگرسیون چندگانه مشخص شد که مقادیر میانگین هندسی قطر ذرات و آهک در عمق اول، دارای ارتباط معنی داری با باند سبز، با R^2 تعدیل شده ۰/۷۸ و در باند مادون قرمز نزدیک ۰/۷۷ بوده و در عمق دوم نیز با باند سبز به مقدار ۰/۵۷ و با باند قرمز به مقدار ۰/۵۹ بوده است. در نهایت مشخص گردید، این دو پارامتر دارای تأثیر چشمگیری بر بازتاب طیفی خاک در منطقه می باشند و می توان با استفاده از داده های ماهواره ای و داده های کمکی (اطلاعات جانبی)، به بررسی آنها در خاک منطقه پرداخت.